DOI: 10.1002/ejic.201100565

Metal Oxidation with N_2O_5: The Nitrosylium Nitrates $(NO)Cu(NO_3)_3$, $(NO)_2[Zn(NO_3)_4]$ and $(NO)_6[Ni_4(NO_3)_{12}](NO_3)_2{\cdot}(HNO_3)$

Steffen Gagelmann,[a] Katja Rieß,[a] and Mathias S. Wickleder*[a]

Keywords: Nitrogen oxides / Structure elucidation / X-ray diffraction / Thermal behavior

The oxidation of copper, zinc and nickel by N_2O_5 led, respectively, to turquoise-coloured single crystals of $(NO)Cu(NO_3)_3$ [monoclinic, $P2_1/m$, $Z = 2$, $a = 465.90(5)$, $b = 1111.7(1)$, $c = 700.7(1)$ pm, $\beta = 100.70(2)°$, $wR_2 = 0.0566$], light-yellow single crystals of $(NO)_2[Zn(NO_3)_4]$ [orthorhombic, $Fdd2$, $Z = 8$, $a = 1522.8(2)$, $b = 2346.4(3)$, $c = 596.18(7)$ pm, $wR_2 = 0.0452$] and green single crystals of $(NO)_6[Ni_4(NO_3)_{12}](NO_3)_2{\cdot}(HNO_3)$ [orthorhombic, $P2_12_12_1$, $Z = 4$, $a = 1167.68(4)$, $b = 1791.97(6)$, $c = 1834.11(6)$ pm, $wR_2 = 0.0762$]. In $(NO)Cu(NO_3)_3$, the Cu^{2+} ion is coordinated by six oxygen atoms of monodentate nitrate groups in the form of a tetragonal distorted octahedron. The nitrate groups are connected to further copper ions leading to a two-dimensional network. In contrast, in $(NO)_2[Zn(NO_3)_4]$, the nitrate anions are coordinated to only one Zn^{2+}, ion and the coordination polyhedron is a distorted octahedron. The complex nitrate $(NO)_6[Ni_4(NO_3)_{12}](NO_3)_2{\cdot}(HNO_3)$ exhibits anionic ribbon chains according to ${}_\infty{}^1\{[Ni(NO_3)_{1/1}(NO_3)_{4/2}]\}_2{}^{2-}$ with octahedrally coordinated Ni^{2+} ions as well as non-coordinating nitrate ions and HNO_3 molecules. The thermal decomposition of the copper and zinc nitrates are multistep processes and lead to a mixture of Cu and Cu_2O in the case of the copper compound and to ZnO for the zinc complex.

Introduction

Investigations of the synthetic potential of dinitrogen tetroxide N_2O_4 and later dinitrogen pentoxide N_2O_5 can be traced back to the work of Addison from the early 1960s. Addison succeeded in preparing a number of nitrosylium nitratometallates, $(NO)_n[M^{m+}(NO_3)_{m+n}]$, which can be decomposed to the corresponding anhydrous nitrates in some cases.[1] Several of these compounds have subsequently been analysed by X-ray diffraction, and – for example – the structures of $(NO)_2[Co(NO_3)_4]$ and $(NO)Mn(NO_3)_3$ have been reported.[2] Our interest in these nitrates was strongly triggered by their potential to function as precursors for the deposition of metals and metal oxides on various surfaces. They seem to be very attractive, because they are carbon-free and should lead to decomposition products without any contamination. One striking example is the compound $(NO_2)[Au(NO_3)_4]$, which we obtained from the reaction of Au with N_2O_5.[3] This compound can be decomposed to elemental gold, induced by the electron beam of an electron microscope. These results encouraged us to perform further reactions of metals with N_2O_5 and to investigate the compounds obtained and their thermal behaviour. In this paper we show that copper and zinc are readily oxidized by N_2O_5 to give the nitrates $(NO)Cu(NO_3)_3$ and $(NO)_2[Zn(NO_3)_4]$ in single-crystalline form. The copper compound was obtained and structurally investigated for the first time in 1973 by the reaction of $Cu(NO_3)_2$ and N_2O_4,[4] and later on by the reaction of $Cu(NO_3)_2$ and fuming HNO_3.[5] In addition to the new preparative route, we describe here its thermal behaviour for the first time. In the reaction of the metal with N_2O_5, the nickel nitrate $(NO)_6[Ni_4(NO_3)_{12}](NO_3)_2{\cdot}(HNO_3)$ is formed instead of the expected copper and zinc congener $(NO)_n[Ni(NO_3)_{2+n}]$, clearly due to a slight contamination of the reaction mixture with water.

Results and Discussion

Crystal Structures

$(NO)Cu(NO_3)_3$ crystallizes in the monoclinic space group $P2_1/m$ with two formula units in the structure cell (Figure 1). The Cu^{2+} ion is situated on a centre of symmetry (Wyckoff symbol 2*c*). One of the nitrate groups, $N(2)O_3^-$, and the nitrosylium ion NO^+ are bisected by a mirror plane (Wyckoff symbol 2*e*).

The copper ion is coordinated by six oxygen atoms belonging to two crystallographically different nitrate groups, $N(1)O_3^-$ and $N(2)O_3^-$. It lies in the centre of an octahedron, which is tetragonally distorted as a result of a Jahn–Teller effect on Cu^{2+} (Figure 2). The axial distances [Cu–O13 253.5(2) pm (2×)] are significantly elongated relative to the equatorial distances [Cu–O21 198.8(2) pm (2×); Cu–O11 194.8(2) pm (2×)]. The octahedron is further distorted with respect to the observed O–Cu–O angles, some of which differ significantly from 90°, that is, the line O13–Cu–O13 defined by the Cu^{2+} ion and the apical oxygen atoms is signifi-

[a] Universität Oldenburg, Institut für Reine und Angewandte Chemie,
Carl von Ossietzky Str. 9–11, 26111 Oldenburg, Germany
E-mail: mathias.wickleder@uni-oldenburg.de

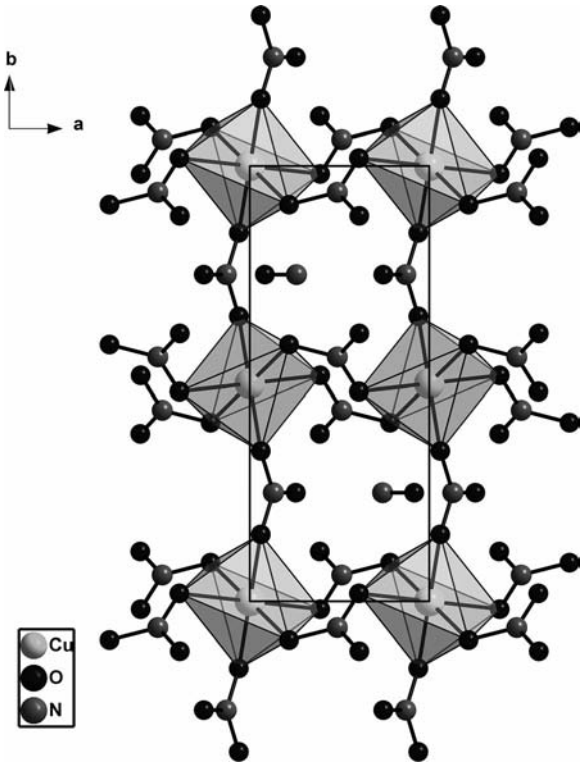

Figure 1. Projection of the crystal structure of $(NO)Cu(NO_3)_3$ onto the (001) plane.

cantly tilted with respect to the square plane defined by the equatorial oxygen atoms O11 and O21.

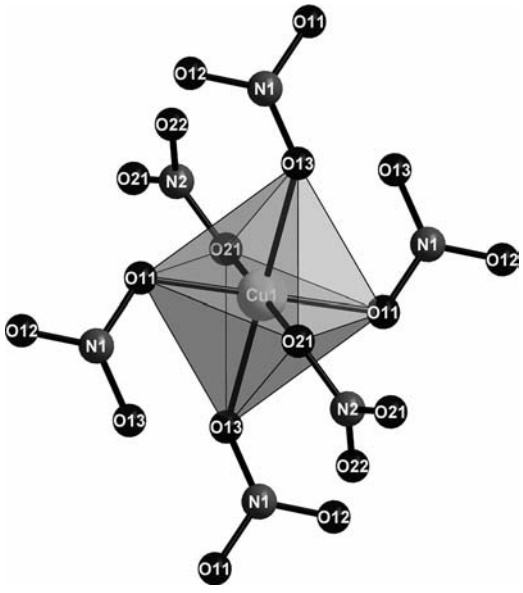

Figure 2. Coordination of the Cu^{2+} ion in the crystal structure of $(NO)Cu(NO_3)_3$.

The copper ions are linked by four bridging $N(1)O_3^-$ groups in the [100] direction and by two $N(2)O_3^-$ ions in the [010] direction. In this way layers of $_\infty^2[Cu(NO_3)_{6/2}]^-$ are formed. The charge balance for the layers is achieved by NO^+ ions, which occupy available sites in the lattice at *y*/*b* = 1/4 and 3/4, respectively. The N–O distance in the NO^+ ion is 99.0(5) pm. This is shorter than the theoretical value but in accordance with the findings for other NO^+-containing salts.[6]

The zinc nitrate $(NO)_2[Zn(NO_3)_4]$ crystallizes in the orthorhombic crystal system with the non-centrosymmetric space group *Fdd*2 and with eight formula units in the unit cell (Figure 3).

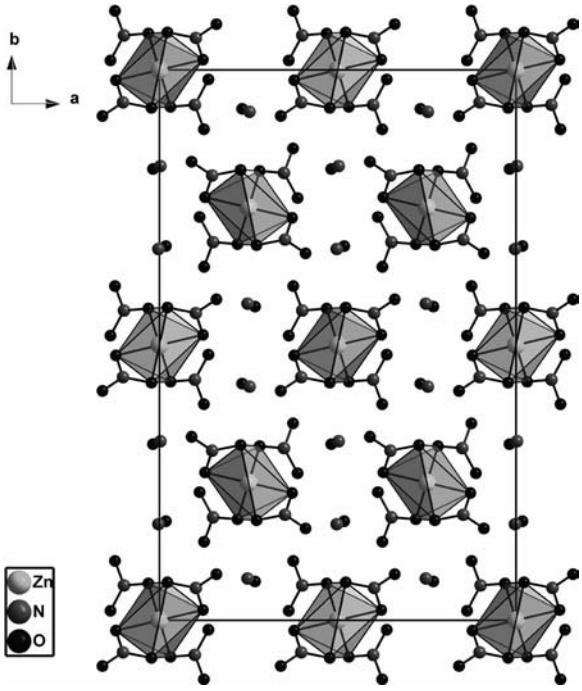

Figure 3. Projection of the crystal structure of $(NO)_2[Zn(NO_3)_4]$ onto the (001) plane.

In contrast to the copper compound, in $(NO)_2[Zn(NO_3)_4]$ the nitrate groups are exclusively coordinated to one Zn^{2+} ion, that is, the complex anion $[Zn(NO_3)_4]^{2-}$ is formed, which is similar in form to the previously observed cesium nitrate $Cs_2[Zn(NO_3)_4]$.[7] Within the anion the zinc atom is surrounded by six oxygen atoms. Four of these oxygen atoms are at shorter Zn–O distances of 201.0(2) pm (2×) and 203.9(2) pm (2×), the remaining two being found at a distance of 236.9(2) pm (2×). The shorter Zn–O distances cause a strongly distorted tetrahedron around the Zn^{2+} ion (Figure 4).

The oxygen atoms belong to two crystallographically different nitrate groups, $N(1)O_3^-$ and $N(2)O_3^-$. The O13–Zn1–O13 angle within the tetrahedron is nearly ideal [108.5(1)°], whereas the O23–Zn1–O23 angle is enlarged up to 138.7(1)°. This results in a widening of one edge of the tetrahedron allowing for additional coordination of the oxygen atom O21. Thus, the nitrate group $N(2)O_3^-$ can be seen as an asymmetrically chelating ligand. The charge of the $[Zn(NO_3)_4]^{2-}$ complex anion is compensated by two nitrosylium ions that belong crystallographically to the same species. The distance between the nitrogen and oxygen atoms within the nitrosylium ion is 104.7(4) pm.

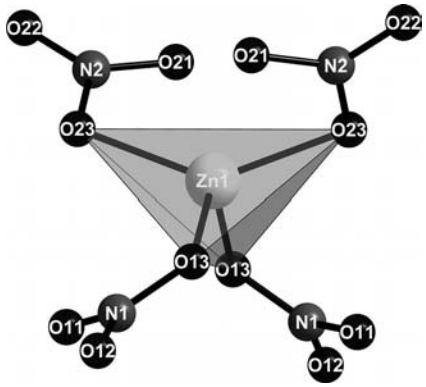

Figure 4. Coordination of the Zn^{2+} ion in the structure of $(NO)_2[Zn(NO_3)_4]$.

The formation of $(NO)_6[Ni_4(NO_3)_{12}](NO_3)_2{\cdot}(HNO_3)$ is clearly a result of a slight contamination by water of the N_2O_5 prepared. The complex crystallizes in the orthorhombic space group $P2_12_12_1$ with four formula units per unit cell. The four crystallographically different Ni^{2+} ions each show the same distorted octahedral coordination of one chelating and four monodentate nitrate groups. Although the Ni–O distances lie in a narrow range from 200.8(5) to 210.0(5) pm, the distortion of the octahedra is especially significant for the O–Ni–O angles involving those oxygen atoms belonging to the chelating nitrate groups (O11, O12, O21, O22, O31, O32, O41, O42), which were found to be between 62.2(2) and 63.2(2)°. The nitrate ions that are bonded in a monodentate fashion can be divided into two categories according to their connectivity modes: two of the four anions act as monodentate bridging ions and lead to a linkage of two $[NiO_6]$ octahedrons to form a dimer (Figure 5).

The remaining two nitrate groups are bidentate bridging ligands and connect the dimers in the [100] direction to form infinite double chains (Figure 6). These can be formu-

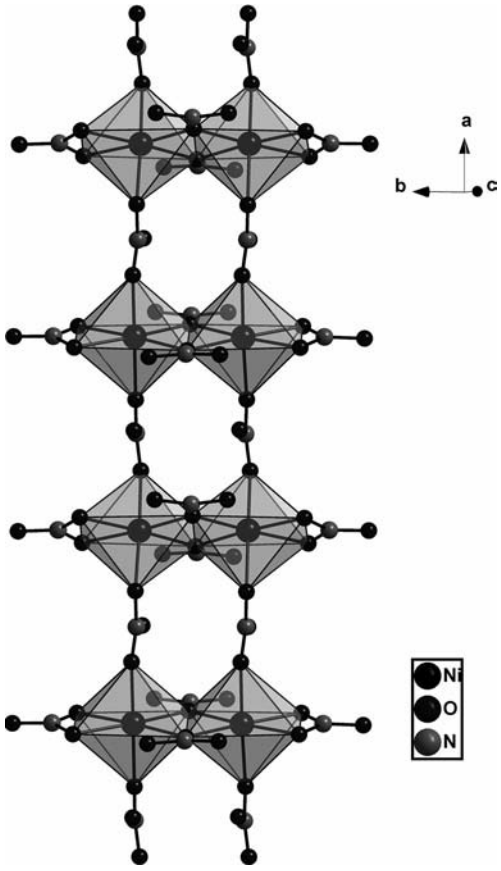

Figure 6. Double chains of $_\infty{}^1\{[Ni(NO_3)_{1/1}(NO_3)_{4/2}]\}_2{}^{2-}$ in $(NO)_6[Ni_4(NO_3)_{12}](NO_3)_2{\cdot}(HNO_3)$.

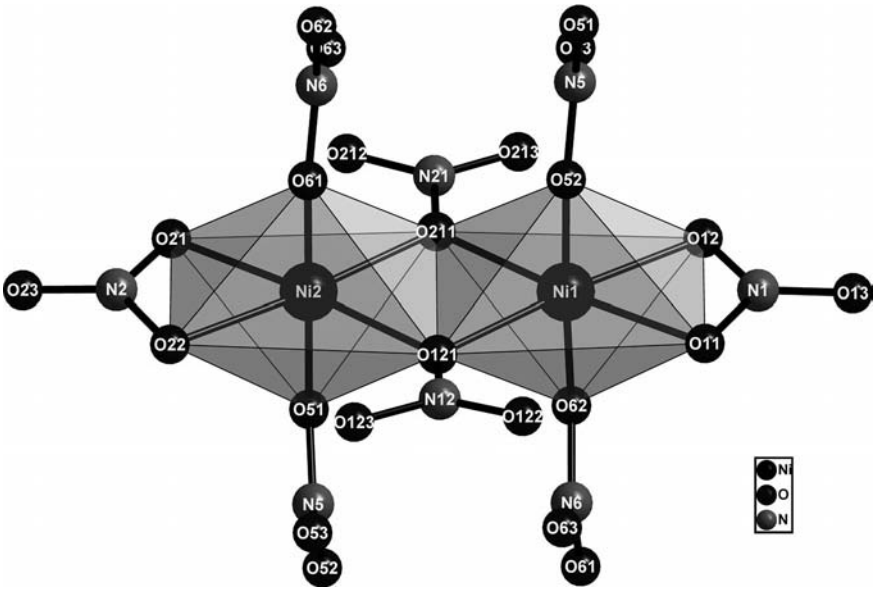

Figure 5. Dimer of two $[NiO_6]$ octahedra in the crystal structure of $(NO)_6[Ni_4(NO_3)_{12}](NO_3)_2{\cdot}(HNO_3)$.

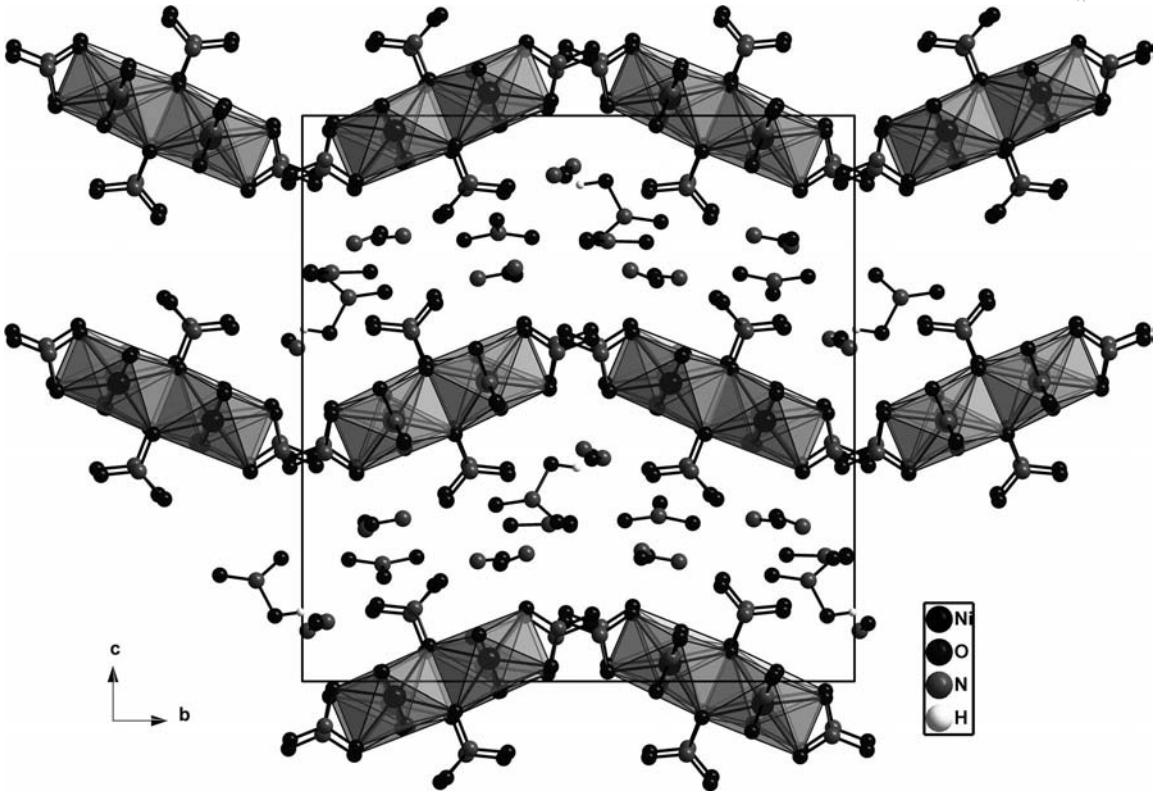

Figure 7. Projection of the crystal structure of $(NO)_6[Ni_4(NO_3)_{12}](NO_3)_2 \cdot (HNO_3)$ onto the (100) plane.

lated as $_{\infty}^{1}\{[Ni(NO_3)_{1/1}(NO_3)_{4/2}]\}_2^{2-}$ according to Niggli's formalism.

The crystal structure exhibits two crystallographically different double chains that show, however, essentially identical bond lengths and angles. The chains are arranged into puckered layers that are stacked in the [001] direction of the unit cell (Figure 7). Between these layers are located non-coordinated nitrate ions as well as the charge-balancing NO^+ ions. The N–O distances for the nitrate ions [123.8(8)–130.2(8) pm] and the nitrosylium cations [96.3(9)–111.4(9) pm] are in accordance with reported values.

Furthermore, the interlayer spacing contains a nitric acid molecule, which can be clearly identified on the basis of the observed N–O distances. These are 120.7(9) and 125.7(8) pm for two of the oxygen atoms and 139.8(8) pm for the third, which indicates the presence of an H atom at this oxygen atom. This is in accordance with the findings for other nitric acid adducts.[8]

Thermal Decomposition

The thermal decomposition of $(NO)Cu(NO_3)_3$ proceeds in at least two steps (Figure 8). The first step has an onset temperature of 115 °C and ends at 183 °C with two endothermic maxima at 118 and 157 °C (Table 1). The product formed in this step is probably $Cu(NO_3)_2$ (mass loss: calcd. 32.9%; found 34.8%). The second step consists of two not well-resolved stages. One significant DTA peak is observed at 286 °C. The overall mass loss for this step is approximately 36%, but there is no distinct plateau in the TG curve. However, it is known that copper nitrate decomposes with the formation of CuO (mass loss: calcd. 39.5%) as an intermediate.[9]

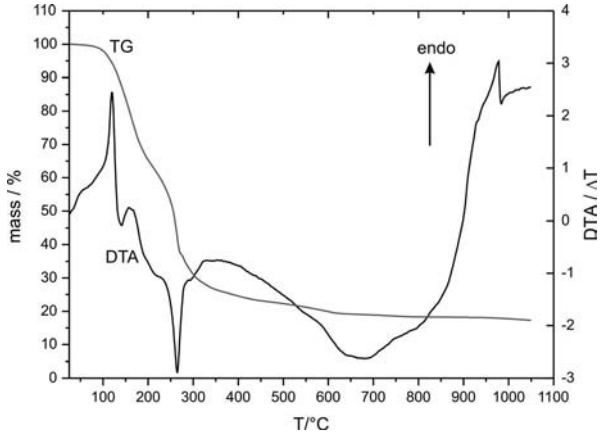

Figure 8. DTA/TG diagram of the thermal decomposition of $(NO)Cu(NO_3)_3$.

Upon further heating, continuous weight loss is observed, but again no plateau occurs in the TG curve. Another endothermic peak at 975 °C is not associated with a loss of mass. On the other hand, the temperature fits well with the temperature reported for the decomposition of CuO to Cu_2O. We assume that gradual degradation of CuO starts after its formation and causes the decline of the TG curve. The final decomposition product is a mixture of

Table 1. Data for the thermal decomposition of $(NO)Cu(NO_3)_3$ and $(NO)_2[Zn(NO_3)_4]$.

Compound	Stage	T_{onset} [°C]	T_{end} [°C]	T_{max} [°C]	Mass loss [%] found	calcd.
$(NO)Cu(NO_3)_3$	1. formation of $Cu(NO_3)_2$ (*endo*)	115	183	118; 157	34.8	32.9
	2. formation of CuO (*exo*)	255	302	286	36.0	39.5
	3. formation of Cu_2O and Cu (*endo*)	950	1010	975	_[a]	10
					75.5	82.4
$(NO)_2[Zn(NO_3)_4]$	1. unknown (*endo*)	61	99	81	18.5	
	2. formation of $(NO)Zn(NO_3)_3$ (*endo*)	120	158	133	8.9	24.5 (steps 1 + 2)
	3. unknown (*endo*)	_[a]			13.9	
	4. formation of ZnO (*endo*)	308	379	342	26.8	42.6 (steps 3 + 4)
					68.1	77.1

[a] Not determined with reliability.

Cu_2O and Cu, as can be seen from the X-ray powder pattern (Figure 9). The complete mass loss was higher than expected for the two decomposition products (Cu: 77.3%; Cu_2O: 74.4%), which may be explained by the difficulties encountered in the sample preparation mentioned above.

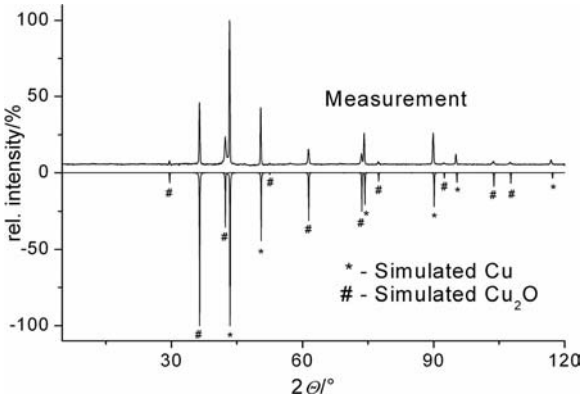

Figure 9. XRD powder diffractogram of the residue of the decomposition product of $(NO)Cu(NO_3)_3$.

The first step of the thermal decomposition of $(NO)_2[Zn(NO_3)_4]$ starts with an onset temperature of 61 °C and finishes at 99 °C (Figure 10). The mass loss of 18.5% is difficult to interpret, but, with the second step, which occurs between 120 and 158 °C, the overall mass loss corresponds to the formula $(NO)Zn(NO_3)_3$. Two further decomposition steps are observed in the TG curve with mass losses of 13.9 and 26.8%, respectively. The corresponding temperatures in the DTA curve are reliable only for the second step.

The overall mass loss is 68.1%, which is also significantly smaller than that calculated for the formation of ZnO as residue, as shown by the X-ray powder pattern (Figure 11). The difference between the observed and calculated mass loss seems reasonable if one takes into account the fact that the initial sample may have contained a significant amount of unreacted N_2O_5. Nevertheless, the suitability of the compound to act as precursor to ZnO has been clearly demonstrated.

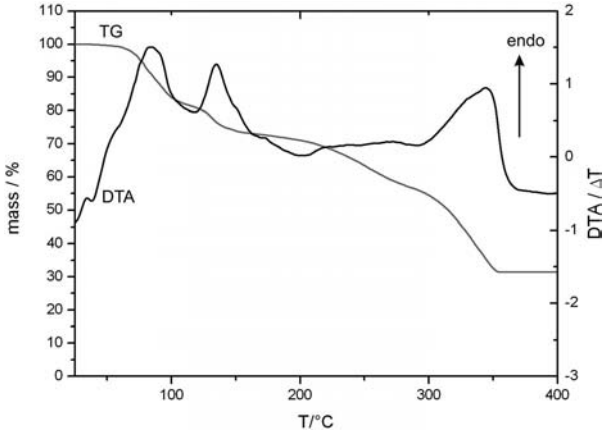

Figure 10. DTA/TG diagram of the thermal decomposition of $(NO)_2[Zn(NO_3)_4]$.

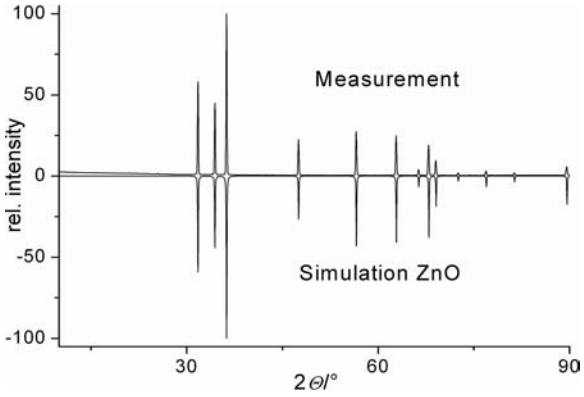

Figure 11. XRD powder diffractogram of the residue of the decomposition product of $(NO)_2[Zn(NO_3)_4]$.

Conclusions

In this paper we have presented the structures and the thermal behaviour of $(NO)Cu(NO_3)_3$ and the new nitrosylium complex $(NO)_2[Zn(NO_3)_4]$. Both compounds were obtained by the reaction of N_2O_5 with the elemental metals. $(NO)Cu(NO_3)_3$ forms a two-dimensional network through bridging nitrato ligands, whereas $(NO)_2[Zn(NO_3)_4]$ contains

discrete nitrate anions. The thermal decomposition of the complexes leads to a mixture of Cu + Cu_2O and ZnO, respectively. We were also able to obtain the unique complex nitrate $(NO)_6[Ni_4(NO_3)_{12}](NO_3)_2 \cdot (HNO_3)$ by the reaction of N_2O_5 with nickel. It consists of double chains of $_\infty^1\{[Ni(NO_3)_{1/1}(NO_3)_{4/2}]\}_2^{2-}$ that are arranged into layers housing NO^+ cations, non-coordinating nitrate ions and free HNO_3 molecules.

Experimental Section

Syntheses: All compounds were obtained by the reaction of N_2O_5 with the metals at room temperature. N_2O_5 was prepared by the reaction of fuming HNO_3 with P_4O_{10} according to a literature procedure.[10] It was directly condensed onto small amounts of ground copper, zinc and nickel powder. The copper compound was prepared in a Schlenk tube at room temperature. The reaction of liquid N_2O_5 with the metal resulted in a green solution after a few days. During the evaporation of unreacted N_2O_5 in a stream of N_2, turquoise-coloured crystals grew. Light-yellow single crystals of the zinc complex grew after several days when the reaction mixture was kept in a sealed glass ampoule. The reaction of nickel powder and N_2O_5 was also performed in a sealed glass tube by heating at 100 °C to yield green single crystals. For copper and zinc, the reactions were almost quantitative with respect to the initial metal content. The reaction with nickel afforded some green crystals (approximately 10–15% based on the initial metal amount), but the yellow-green solution indicated that there was still some metal dissolved. Concentration of this solution after recovering the green crystals led to a yellow powder of low crystallinity and unknown composition. All compounds are very moisture-sensitive and have to be handled under a protective gas. Crystals of $(NO)_6[Ni_4(NO_3)_{12}](NO_3)_2 \cdot (HNO_3)$ turned cloudy and changed to a brown-yellow colour even in a glovebox so that no further characterization has been performed on this compound.

IR Spectroscopy: IR spectra were recorded in the range of 600–4000 cm^{-1} with a Bruker Tensor 27 spectrometer equipped with a "GoldenGate" diamond-ATR unit. $(NO)Cu(NO_3)_3$: $\tilde{\nu}$ = 2340 (m), 1538 (m), 1423 (s), 1330 (s), 1290 (s), 1040 (m), 1010 (m), 800 (m), 790 (s), 710 (s) cm^{-1}. $(NO)_2[Zn(NO_3)_4]$: $\tilde{\nu}$ = 2310 (m), 1575 (s), 1364 (m), 1298 (s), 955 (sh), 905 (s), 792 (m), 767 (m), 702 (m) cm^{-1}.

X-ray Crystallography: Appropriate crystals of the compounds were selected, and diffraction data were collected by using an image plate diffractometer (IPDS I, STOE & CIE) and CCD diffractometer (Kappa APEX II, Bruker). The structures were solved successfully by direct methods by the program SHELXS-97 assuming the space group $P2_1/m$ for the copper complex, $Fdd2$ for the zinc complex and $P2_12_12_1$ for the nickel compound.[11] For the subsequent full-matrix least-squares refinement, the program SHELXL-97 was used.[12] A numerical absorption correction was applied to the data with the help of the programs X-RED and X-SHAPE.[13,14] The data are summarized in Table 2. Further details on the crystal structure investigations may be obtained from the Fachinformationszentrum Karlsruhe, 76344 Eggenstein-Leopoldshafen, Germany (Fax: +49-7247-808-666; E-mail: crysdata@fiz-karlsruhe.de), on quoting the depository numbers CSD-422032 {for $(NO)_2[Zn(NO_3)_4]$}, -422033 [for $(NO)Cu(NO_3)_3$] and -422792 {for $(NO)_6[Ni_4(NO_3)_{12}](NO_3)_2 \cdot (HNO_3)$}.

Thermal Analysis: DTA/TG measurements for $(NO)Cu(NO_3)_3$ and $(NO)_2[Zn(NO_3)_4]$ were performed by using a thermal analyser (TGA/SDTA 851^e, Mettler-Toledo). For this purpose, about 10 mg of the substance was placed in a corundum container. The samples were prepared in a glove box due to the extreme moisture sensitivity of the compounds. Nevertheless, for the zinc compound, the complete removal of all traces of N_2O_5 was not possible due to its sensitivity. The samples also had to be protected during the transfer to the thermoanalyser. The corundum crucibles were heated at a constant rate of 10 K/min under a flow of nitrogen, and the thermal decomposition was monitored from 25 to 1050 °C. Characteristic points such as the onset and end temperatures of the thermal

Table 2. Crystallographic data for $(NO)Cu(NO_3)_3$, $(NO)_2[Zn(NO_3)]_4$ and $(NO)_6[Ni_4(NO_3)_{12}](NO_3)_2 \cdot (HNO_3)$.

	$(NO)Cu(NO_3)_3$	$(NO)_2[Zn(NO_3)_4]$	$(NO)_6[Ni_4(NO_3)_{12}](NO_3)_2 \cdot (HNO_3)$
Crystal size [mm]	0.30 × 0.07 × 0.05	0.44 × 0.54 × 0.60	0.14 × 0.07 × 0.02
Molar mass [g/mol]	279.58	373.43	1346.06
Crystal system	monoclinic	orthorhombic	orthorhombic
Space group	$P2_1/m$ (No. 11)	$Fdd2$ (No. 43)	$P2_12_12_1$ (No. 19)
a [pm]	465.90(5)	1522.8(2)	1167.68(4)
b [pm]	1111.7(1)	2346.4(3)	1791.97(6)
c [pm]	700.7(1)	596.18(7)	1834.11(6)
β [°]	100.70(2)		
Cell volume	356.62(7)	2130.2(5)	3837.8(2)
No. of formula units	2	8	4
Temperature [K]	153	153	153
Radiation	Mo-K_α	Mo-K_α	Mo-K_α
λ [pm]	71.07	71.07	71.07
μ [mm^{-1}]	3.131	2.416	2.121
Extinction coefficient	–	0.0002(1)	–
Measured reflections	4294	6258	53559
Unique reflections	706	1068	6745
with $I_o > 2\sigma(I)$	581	979	3838
R_{int}/R_σ	0.0332/0.0249	0.0633/0.0342	0.0960/0.0944
R_1, wR_2 [$I_o > 2\sigma(I)$]	0.0230; 0.0551	0.0222; 0.0448	0.0398; 0.0762
R_1, wR_2 (all data)	0.0308; 0.0566	0.0251; 0.0452	0.0841; 0.0856
Goodness of fit	1.044	1.496	0.810
Flack x parameter	–	0.24(1)	0.16(2)

effects were taken from the DTA curve according to common procedures by using the software delivered with the analyser.[15] The data are summarized in Table 1. The residues of the decomposition reactions were investigated by X-ray powder diffraction (STADI P, STOE & CIE); the samples were prepared on a flat sample holder, and the diffraction patterns were analysed by using the diffractometer's software.[16]

Acknowledgments

The authors are grateful to Wolfgang Saak for collecting the X-ray data.

[1] C. C. Addison, *Chem. Rev.* **1980**, *80*, 21–39.
[2] G. A. Tikhomirov, K. O. Znamenkov, I. V. Morozov, E. Kemnitz, S. I. Troyanov, *Z. Anorg. Allg. Chem.* **2002**, *628*, 269–273.
[3] M. S. Wickleder, O. Büchner, F. Gerlach, M. Necke, K. Al-Shamery, T. Wich, T. Lutterman, *Chem. Mater.* **2008**, *20*, 5181–5185.
[4] L. J. Blackwell, T. J. King, A. Morris, *J. Chem. Soc., Chem. Commun.* **1973**, *17*, 644–644.
[5] K. O. Znamenkov, I. V. Morozov, S. I. Troyanov, *Zh. Neorg. Khim.* **2004**, *49*, 213–220.
[6] Z. Mazej, M. Ponikvar-Svet, J. F. Liebman, J. Passmore, H. D. Brooke Jenkins, *J. Fluorine Chem.* **2009**, *130*, 788–791.
[7] I. V. Morozov, E. Kemnitz, S. I. Troyanov, *Z. Anorg. Allg. Chem.* **1999**, *625*, 1664–1699.
[8] M. D. Moran, D. S. Brock, H. P. A. Mercier, G. J. Schrobilgen, *J. Am. Chem. Soc.* **2010**, *132*, 13823–13839.
[9] R. Nikolic, S. Zec, V. Maksimovic, S. Mentus, *J. Therm. Anal. Calorim.* **2006**, *86*, 423–428.
[10] B. O. Field, C. J. Hardy, *Q. Rev. Chem. Soc.* **1964**, *18*, 361–388.
[11] G. M. Sheldrick, *SHELXS-97 – Program for Solution of Crystal Structures*, University of Göttingen, Göttingen, **1997**.
[12] G. M. Sheldrick, *SHELXL-97 – Program for the Refinement of Crystal Structures*, University of Göttingen, Göttingen, **1997**.
[13] *X-RED 1.22 – Program for Data Reduction for STADI4 and IPDS*, Stoe & Cie, Darmstadt, **2001**.
[14] *X-SHAPE 1.06 – Program for Crystal Optimisation for Numerical Absorption Correction*, Stoe & Cie, Darmstadt, **1996**.
[15] *STAR^e*, Software for control of DTA/TGA apparatus and evaluation of measurement data, Mettler-Toledo GmbH, Schwerzenbach, **2004**.
[16] *VISUAL X^{POW} 3.01*, software package for the STOE powder diffraction system, Stoe & Cie, Darmstadt, Germany, **1996**.

Received: June 3, 2011
Published Online: October 14, 2011

